Chapter 2

Literature Survey

2.1 Introduction

In this chapter, a comprehensive literature survey of linearly and circularly polarized PRA designs is presented. It begins with the description of techniques used to achieve 1-D and 2-D beam steering. The main focus of this review is given on parasitic antenna designs. Then, the existing state-of-the-art techniques used to achieve beamwidth reconfiguration are described. The RA designs realizing beam steering and beamwidth reconfiguration in the single antenna structure are also discussed. Finally, the RA designs capable of achieving pattern reconfiguration along with polarization reconfiguration are reviewed in detail.

2.2 Literature Review

The research work on PRA has been carried out in areas by changing the main lobe direction, varying 3-dB beamwidth, or combining these two characteristics. PRA designs reported in the literature are classified according to their radiation capabilities such as 1-D beam steering, 2-D beam steering, beamwidth RA, and beam steering and beamwidth RA, as shown in Figure 2.1. The pattern and polarization RA designs are classified based on the pattern reconfiguration characteristics, as shown in Figure 2.2. In the first case, antenna designs radiating in different directions and producing different beam shapes are described. In the second case, antenna designs achieving beam steering with polarization reconfiguration are discussed in detail.

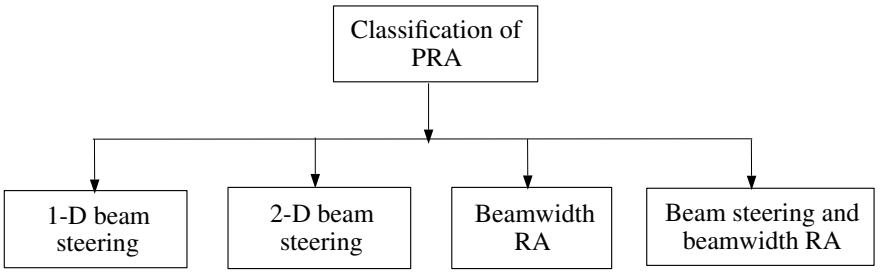

Figure 2.1. Classification of PRA.

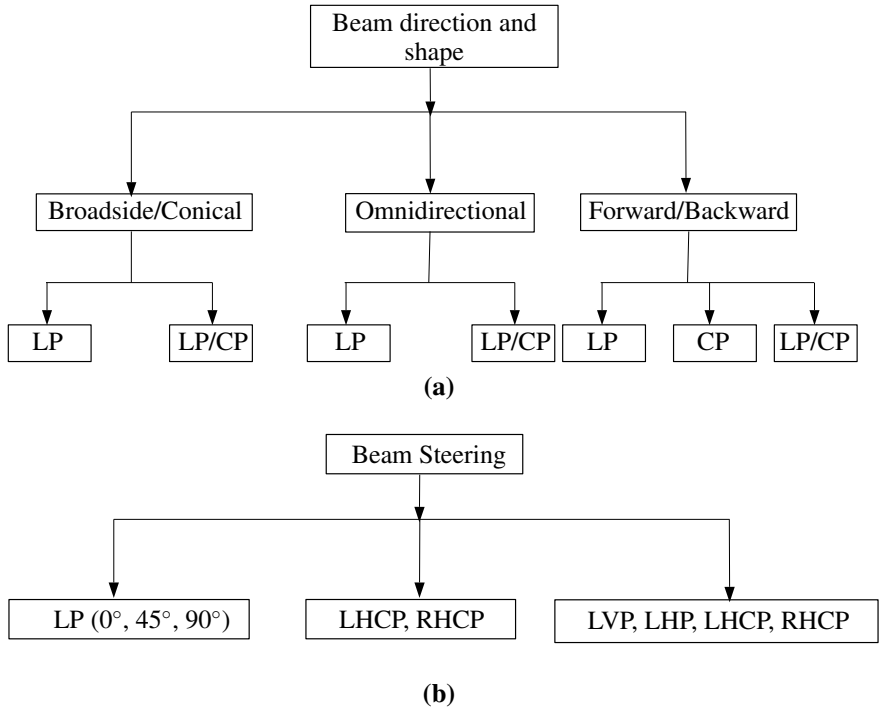

Figure 2.2. Classification of reported pattern and polarization RA designs based on (a) Direction and shape of the radiated beam and (b) Beam steering.

2.2.1 One-Dimensional (1-D) Beam Steering Reconfigurable Antenna

To steer main beam of the antenna, various techniques are proposed in the literature such as metamaterial-based structures [38, 39], tunable materials [40], Leaky Wave Antenna (LWA) [41, 42], Partially Reflective Surface (PRS) [43] and parasitically coupled antenna elements [6, 44–57].

A Dielectric Resonator Antenna (DRA) with a negative refractive index metamaterial is proposed in [38] to achieve a beam deflection of $\pm 38°$. In [39], by tuning parameters of Complementary Split Ring Resonator (CSRR) structure, the beam can be steered from $-51°$ to $48°$. A ferrite loaded microstrip antenna reported in [40] scans the main beam from $-26°$ to $28°$. The LWA using Electromagnetic Band Gap (EBG) structure in [41] and tunable High Impedance Surface

(HIS) in [42] is reported to realize continuous beam scanning from -25° to 25° and 9° to 30° respectively. A PRS with an aperture coupled feed radiates in the 0° and $\pm 15^\circ$ directions [43].

The concept of microstrip Yagi is proposed by Huang and Densmore, which consists of one driven patch, one reflector element, and two director patches [45]. The main beam of the microstrip Yagi antenna is discretely switched or continuously scanned depending upon the switching mechanism used in the antenna structure. The antenna designs presented in [6, 46–49] makes use of PIN diodes to achieve discrete beam switching. A pattern reconfigurable parasitic array presented in [6] switches the main beam to -35°, 0° and 35°. A quasi-Yagi antenna in [46] tilts the main beam in directions -20°, 0° and 20°. A reconfigurable parasitic antenna is designed in [47] to achieve discrete beam switching in directions -30°, 0° and 30° using PIN diodes. In [48], the ground plane truncation method is proposed to improve beam switching capabilities of the parasitic antenna. However, this method suffers from drawbacks, such as high Side Lobe Level (SLL) and low gain at increased beam tilt angles. A multilayer parasitic pixel antenna presented in [49] radiates in the directions -30°, 0° and 30°.

Continuous beam scanning is realized by using capacitors in [50–52] and varactor diodes in [44, 55–57]. In [50], the radiated beam is continuously scanned from -20° to 20° by changing the reactance of capacitors loaded on the parasitic elements. In [51], a similar method is used to realize beam scanning from -15° to 15°. In [52], DRA elements are employed to achieve beam scanning from -30° to 30°. In [44], radiated beam is continuously scanned from -36° to 32° with CP characteristics. However, the performance of this antenna is tested with only one tunable parasitic element. Harrington proposed the theory of reactively controlled directive arrays using a driven dipole and tunable parasitic elements in [53]. Authors in [54] used this theory to propose ESPAR antennas. A multilayer ESPAR antenna presented in [55] scans the main beam from -15° to 15°. This antenna design is further extended in [56] to form 2×2 ESPAR array, which achieves continuous beam scanning from -20° to 20° with boresight gain of 12.1 dBi. In [57], five-element microstrip Yagi design is presented to realize continuous beam scanning from -24° to 24°.

Table 2.1 presents a detailed comparison of the PRA designs performing 1-D beam steering. It is worth noting that,

- Reported designs in [6, 46, 47, 49] achieve discrete beam switching and small beam deflection angle.
- Antenna designs presented in [44, 50–52, 55–57] realize continuous beam steering, but the scanning range is limited to -36° to 32°.
- The use of capacitors in [50–52] makes it difficult for real-time beam scanning.

Table 2.1. Performance comparison of the PRA designs achieving 1-D beam steering.

Ref.	Antenna type	Operating frequency (GHz)	Main beam elevation plane (degree)	−10 dB bandwidth (%)	Peak gain (dBi)	Substrate	Size (mm^3)	Switches (number)	Steering type
[6]	Parasitic strips	3.65	−35, 0, 35	5.18	n/a	n/a	n/a	copper strips (4)	discrete
[46]	Quasi-Yagi dipole	5.2	−20, 0, 20	6.76	10.03	Rogers	110×70×1.27	PIN (12)	discrete
[47]	Parasitic with shorting pin	5.8	−30, 0, 30	2.79	6.5	Taconic	48×22.6×1.6	PIN (2)	discrete
[48]	Parasitic patch with ground plane truncation	5.8	−50, −30, 0, 30, 50	4.2	7.5	Taconic	108×36×1.6	PIN (6)	discrete
[49]	Parasitic pixel layer	5.5	−30, 0, 30	15	6.5	Rogers	60×67×15.081	PIN (2)	discrete
[50]	Tunable parasitic	3	−20 to 20	1.8	n/a	Rogers	n/a	capacitor (2)	continuous
[51]	Tunable parasitic	2.45	−15 to 15	2.06	8	Rogers	192×76.8×1.6	capacitor (4)	continuous
[52]	Parasitic DRA	2.8	−30 to 30	4.6	7.5	Rogers	n/a	capacitor (2)	continuous
[44]	Tunable parasitic	2.45	−36 to 32	2	8.1	Rogers	150×100×3.175	varactor (4)	continuous
[55]	ESPAR	1	−15 to 15	n/a	7.4	Rogers	n/a	varactor (8)	continuous
[56]	ESPAR 2×2 array	1	−20 to 20	n/a	12.1	Rogers	n/a	varactor (32)	continuous
[57]	Tunable parasitic	0.8665	−24 to 24	0.35	6	Arlon	500×150×3.18	varactor (2)	continuous

2.2.2 Two-Dimensional (2-D) Beam Steering Reconfigurable Antenna

A 2-D (azimuth and elevation) beam steering is achieved by various techniques such as LWA array [58], holographic antennas [59], electrically tunable impedance surface [60], Frequency Selective Surface (FSS) [61], parasitic antenna design [62], Fabry-Perot antenna [63], antenna with metamaterial slab [64], Substrate Integrated Waveguide (SIW) [65], CSRR [66] and patch-slot-ring structure [67].

To enhance radiation capabilities of the parasitic antenna in azimuth and elevation plane, various designs are reported in the literature based on reactive loads [68–72], size-tunable parasitic elements [62], shorting pin [73–75], tapered microstrip stubs [76, 77], switchable director/reflector [78], parasitic pixel layer [24, 79], edge-grounded sector patches [80] and dipole with parasitic striplines [81].

An ESPAR design is reported in [68] using variable reactive loads to achieve beam scanning of $\pm 9^\circ$ and $\pm 16^\circ$ in the E-plane and H-plane respectively. A cavity-backed slot ESPAR cross array is proposed in [69] to achieve independent beam scanning in the E-plane from -24° to 24° and in the H-plane from -20° to 20°. In [70], a large array of DRA is designed in X-band based on the ESPAR concept. The performance of this antenna is compared with beam steerable reflectarray antenna and a traditional phased array antenna. It is concluded that the proposed ESPAR DRA is able to reduce the number of phase shifters by 80% in comparison with the conventional phased array. A cross parasitic array antenna is presented in [71], to obtain beam scanning up to 30° by terminating parasitic elements with varactors. In [72], the parasitic elements loaded with reactance devices are placed in the X (diagonal) configuration to achieve complete azimuthal beam scanning. In [62], two tunable parasitic elements are employed to attain continuous beam scanning in the elevation plane from $\theta = 0^\circ$ to 32° for $\phi = 0^\circ$, 45° and 90° planes.

In [73], a circular parasitic structure is utilized along with shorting pins to realize discrete beam switching in $\phi = 0^\circ$, 45°, 135°, 225° and 315° planes. In [76], a combination of circular disc and microstrip stubs are used to achieve beam switching in $\phi = 0^\circ$, 90°, 180° and 270° planes with a beam tilting of 36°. A wideband pattern RA proposed in [78] consists of two radial radiators, a truncated ground plane and, two parallel strips placed around the radiators. The main beam of this antenna is steered in four directions $\phi = 0^\circ$, 45°, 135° and 180° in the azimuth plane.

In [74], a similar principle is used as that of [73] to radiate the main beam in nine angular directions with an elevation angle of 25°. A circular disc and switch controlled tapered strips achieve a complete azimuthal beam switching with a maximum elevation angle of 36° in [77]. In [24] and [79] parasitic pixel layer is used to cover the complete azimuth plane with the main beam

switched to 30° and 40° respectively in the elevation plane. A PRA consisting of a radiating dipole with switchable parasitic strip lines is proposed in [81]. The main beam of this antenna can be switched in the elevation plane from left endfire to right endfire along with boresight radiation. The symmetrical antenna structure comprised of a circular patch, edge-grounded sector-patches, and parasitic strips are developed in [80] to accomplish 360° beam scanning in the azimuth plane with scanning step of 60°. The RA design reported in [75] achieves 360° beam steering in the azimuth plane by controlling a switching state of the shorting switch connected to the radiation patch and parasitic elements.

Table 2.2 presents a detailed performance comparison of 2-D beam steering PRAs. It is observed that,

- The designs reported in [62, 67–69, 73, 76, 78] are unable to cover the complete horizontal plane.
- Antenna designs presented in [71, 72] has the advantage of achieving complete azimuthal beam scanning. However, in [71], priority is given to SNR rather than to maintaining low return loss. It would be challenging to integrate this antenna into a larger array considering poor impedance matching. Also, in [72] complex biasing circuit is required to achieve desired reactance values.
- The parasitic pixel layer used in [79] needs a large number of RF switches and chokes, which increases complexity of the DC biasing network.

Table 2.2. Performance comparison of the PRA designs achieving 2-D beam steering.

Ref.	Antenna type	Operating frequency (GHz)	Azimuth plane coverage (degree)	Main beam elevation plane (degree)	−10 dB bandwidth (%)	Peak gain (dBi)	Substrate	Size (mm^3)	Switches (number)	Steering type
[67]	Patch-slot-ring	2.05	E & H	±22	2.6	4.58	FR4	175×170×7.52	PIN (4)	discrete
[68]	ESPAR	n/a	$\phi = 0$ $\phi = 90$	±30 ±20	n/a	n/a	Rogers	n/a	varactor (2)	continuous
[69]	Cavity-backed slot ESPAR	4.1	$\phi = 0$ $\phi = 90$	−24 to 24 −20 to 20	n/a	n/a	Rogers	n/a	varactor (4)	continuous
[62]	Parasitic	2.5	ϕ = 0, 45, 90	0 to 32	n/a	8.51	Rogers	150×150×3.175	varactor (2)	continuous
[73]	Parasitic	2.38	ϕ = 0, 45, 135, 225, 315	0, 13, 15, 10, 12	1.68	8.2	Taconic	130×130×1.57	PIN (4)	discrete
[76]	PIN controlled stubs	2.45	ϕ = 0, 90, 180, 270	35	4.88	5	FR4	50×50×6.4	PIN (4)	discrete
[78]	Switchable director/reflector	1.88	ϕ = 0, 45, 135, 180	n/a	34	3.7	FR4	36×48×1.6	PIN (4)	discrete
[65]	SIW horn	5	360	22.5	26.2	10	Rogers	37 (diameter) 3.175 (thickness)	PIN (64)	discrete
[66]	CSRR on ground plane	2.45	360	±31	2.45	7.2	$\epsilon_r = 2.5$	100×95.5×3	PIN (8)	discrete

Continued on next page

Table 2.2 – *Continued from previous page*

Ref.	Antenna type	Operating frequency (GHz)	Azimuth plane coverage (degree)	Main beam elevation plane (degree)	−10 dB bandwidth (%)	Peak gain (dBi)	Substrate	Size (mm^3)	Switches (number)	Steering type
[72]	Reactively loaded parasitic	5	360	40	4	9.4	PTFE	96×96×2.35	reactive loading	continuous
[74]	Parasitic	2.38	360	25	1.26	8.01	Taconic	120×120×1.6	PIN (4)	discrete
[77]	PIN controlled strips	2.4	360	36	10.48	4.5	FR4	40×40×6.4	PIN (8)	discrete
[24]	Parasitic pixel layer	2.45	360	30	4.08	6.5	Rogers	90×98×12.7	PIN (12)	discrete
[79]	Parasitic pixel layer	5.7	360	±40	4	9.5	Rogers	60×42×2.032	hardwired connections (54)	discrete
[81]	Dipole with parasitic striplines	2.45	360	n/a	n/a	6.5	Rogers	70×55×31	PIN (20)	discrete
[80]	Circular patch with edge grounded sector	5.8	360	24	7	8.1	Rogers	40 (diameter) 7.15 (thickness)	PIN (12)	discrete
[75]	Parasitic elements	5.5	360	30	14.5	10	Rogers	45.2 (diameter) 3.82 (thickness)	PIN (2)	discrete

2.2.3 Beamwidth Reconfigurable Antenna

Recently, a great deal of attention has been given to beamwidth RA. Dynamic control over beamwidth of the antenna improves the coverage and traffic capacity of the wireless networks. The beamwidth RAs are highly suitable for cellular base station applications, which demand antennas of different beamwidths for diverse environments [82]. Beamwidth RAs proposed in the literature are based on Magnetoelectric (ME) dipole [82–87], PRS [88–90], tunable parasitic elements [91–93], array structure [94–96], slotted patch [97], FSS [98] and dipole [99].

A linearly polarized three-element ME dipole antenna array is reported in [83] to accomplish beamwidth reconfiguration in the H-plane. The 3-dB beamwidth of this antenna can be discretely switched between 37° and 136° in the H-plane. Limitations of this antenna in terms of discrete beamwidth tuning and beamwidth reconfiguration with single-polarization are overcome in [84] by achieving continuous beamwidth tuning in the H-plane from 80° to 160° with LP and from 72° to 133° with dual orthogonal polarization. A ME dipole antenna in [85] uses tunable strip grating reflector to attain beamwidth reconfiguration in H-plane from 81° to 153°. The ME dipole antenna array developed in [86] realizes beamwidth reconfiguration in the E-plane and H-plane from 24° to 97° and 22° to 100° respectively. It is observed that the earlier reported ME dipole antennas achieve beamwidth reconfiguration in either E-plane or H-plane individually. In [87], the ME dipole antenna with the capability of individual and simultaneous beamwidth reconfiguration is proposed. Beamwidth of this antenna can be continuously tuned in the E-plane, H-plane, and both the E-plane and H-plane from 65° to 120°, 80° to 120°, and 65° to 130° respectively.

The antenna design proposed in [88] uses a cylindrical EBG structure to achieve reconfigurable elevation beamwidth. In [89], the reflection magnitude of the PRS antenna is controlled to achieve beamwidth reconfiguration. A PRS antenna design enabling 1-bit dynamic beamwidth control is presented in [90]. This antenna achieves an 18° and 23° variation of 3-dB beamwidth in the E-plane and H-plane, respectively.

In [91], the parasitic elements are used to control azimuth beamwidth with single or dual LP. In [92] and [93], tunable parasitic elements are used to achieve continuous beamwidth tuning in H-plane and both the principal planes, respectively. The antenna performance in [92] shows a dynamic control over radiation beamwidth that ranges from 50° to 112° with a capacitance tuning range of 0.5 to 2.5 pF. In [93], beamwidth of the RA is continuously tuned from 50° to 141° and 53.8° to 149° in the E-plane and H-plane respectively.

A variable beamwidth 2×2 antenna array that can tune its beamwidth approximately from 65° to 100° is proposed in [94]. A planar microstrip series-fed slot antenna array is proposed in [95],

which provides 2-D beamwidth switching capability. The 3-dB beamwidth in E-plane and H-plane can be tuned from (35°, 65°) to (15°, 31°). The antenna design proposed in [96] consists of a coupler, three reconfigurable output ports, and 1×3 rectangular patch array. This antenna achieves a broad beamwidth of 66.2° and a narrow beamwidth of 24.1°.

A coplanar slotted-patch antenna is presented in [97] to realize broadside radiation with H-plane 3-dB beamwidth of $130°\pm10°$ and $55°\pm1°$. A FSS based antenna controls the E-plane beamwidth from 13.2° to 31.1° at an operating frequency of 5.5 GHz [98]. A reconfigurable dipole antenna presented in [99] achieves beamwidth reconfiguration in the E-plane. The 3-dB beamwidth is switched in three different modes narrow (77.6°), middle (90.7°) and wide (168.3°).

Table 2.3 presents a detailed comparison of beamwidth RA designs reported in the literature. It is observed that,

- The beamwidth RA designs suffer from either narrow bandwidth [87, 89, 92, 99] or narrow tunable beamwidth [90, 95, 98].
- Beamwidth RA designs based on the ME dipole are non-planar and large in size [83–86].
- The methodologies reported in [83, 85, 86, 88, 90, 94, 96, 97, 99] do not provide continuous tuning of beamwidth, as they depend on switching mechanisms.
- The antenna designs presented in [88, 89, 98] need many switches that make biasing circuit integration challenging.
- In some of the designs, beamwidth reconfigurability is achieved only in H-plane [83–85, 92, 94, 96, 97] or E-plane [88, 98, 99].
- There are limited antenna designs reported in the literature which achieve beamwidth reconfiguration in both the principal planes with dual orthogonal LP [86, 90].

Table 2.3. Performance comparison of the RA designs achieving beamwidth reconfigurability.

Ref.	Antenna type	Operating frequency (GHz)	−10 dB bandwidth (%)	3-dB beamwidth (degree)	Plane	Peak gain (dBi)	Switches (Number)	Beamwidth variability	Polarization
[83]	ME dipole	1.9	15	37 to 136	H	9.8	switch (2)	discrete	linear
[84]	ME dipole	2	10	80 to 160 (LP) 72 to 133 (Dual LP)	H	7.1	varactor (2)	continuous	dual linear
[85]	ME dipole	1.9	40	81 to 153	H	6.4	PIN (15)	discrete	linear
[86]	ME dipole	2.7	78.4	22 to 100 24 to 97	E H	11.5	switch (2)	discrete	dual linear
[87]	ME dipole	2.05	4.87	65 to 120 80 to 120 65 to 130	E H E, H	5.8	varactor (4)	continuous	linear
[88]	PRS	2	8	25 to 83	E	6.3	PIN (68)	discrete	n/a
[89]	PRS	2	5	21 to 29.5 24 to 37	E H	15.1	varactor (100)	continuous	linear
[90]	PRS	11.2	n/a	16 to 34 16 to 39	E H	n/a	MEMS	discrete	dual linear
[92]	Tunable parasitic	2.475	2	50 to 112	H	8.6	varactor (2)	continuous	linear

Continued on next page

Table 2.3 – *Continued from previous page*

Ref.	Antenna type	Operating frequency (GHz)	−10 dB bandwidth (%)	3-dB beamwidth (degree)	Plane	Peak gain (dBi)	Switches (Number)	Beamwidth variability	Polarization
[93]	Tunable parasitic	2.4	n/a	50 to 141 53.8 to 149	E H	n/a	varactor (4)	continuous	linear
[94]	Array	2.4	n/a	65 to 100	H	7.36	copper strips (2)	discrete	linear
[95]	Slot antenna array	2.4	2.5 5.8 10.8	15, 31 20, 45 35, 65	E, H	14.5 12.1 7	varactor (1)	continuous	linear
[96]	Array	0.915	n/a	24.1, 66.2	H	11.3	PIN (4)	discrete	n/a
[97]	Slotted patch	2.3	16.24	130, 55	H	5.3, 8.6	PIN (6)	discrete	linear
[98]	FSS	5.5	n/a	13.2 to 31.1	E	19	varactor (96)	continuous	n/a
[99]	Dipole	2.6	4.8	77.6, 90.7, 168.3	E	n/a	PIN (4)	discrete	n/a

2.2.4 Beam Steering and Beamwidth Reconfigurable Antenna

As discussed in Section 2.2.3, most of the beamwidth RAs achieve unidirectional radiation characteristics. However, main beam of the antenna cannot be steered. Several antenna designs are reported in the literature to realize continuous beam scanning and tunable beamwidth in a single antenna structure [25, 100–104]. Techniques used to achieve these objectives are PRS [100], metamaterial [101], antenna with metal walls [102], tunable parasitic elements [103, 104] and parasitic pixel layer [25].

A PRS antenna is proposed in [100] to obtain independent beam scanning and dynamic beamwidth control. Beam scanning is realized from 15° to 20°, and beamwidth is tuned from 18.7° to 22.4°. A metamaterial-based LWA is proposed in [101] to attain tunable radiation angle and beamwidth functionalities. This antenna achieves continuous beam scanning from $-49°$ to 50° at an operating frequency of 3.33 GHz. Continuous beam scanning is accomplished by uniformly biasing varactor diodes. Varactor diodes are non uniformly biased to realize beamwidth tuning.

An aperture-feed PRA with metal walls is presented in [102]. This antenna achieves boresight radiation with narrow and wide beamwidth. Main beam of the antenna is discretely switched in the E-plane and H-plane from $-51°$ to 54° and $-20°$ to 20° respectively. The reflector and director properties of the parasitic elements are used in [103] to achieve beamwidth tuning from 60° to 130° and main lobe scanning from $-20°$ to 20° in the H-plane. A parasitic pixel layer-based RA design is developed in [25] to provide pattern and beamwidth variability on a single antenna structure. This RA generates nine beam steering and three beamwidth variable modes. The antenna covers complete azimuth plane and the main beam is discretely switched to 40° in the elevation plane. This antenna achieves narrow and broad beamwidth of 40° and 100°, in ϕ = 45°, 90° and $-45°$ planes. A low profile dual-polarized PRA is presented in [104]. Main beam of the antenna is directed to 14°, $-17°$ and $-3°$ with narrow beamwidth. This antenna achieves narrow beamwidth of 49° and a wide beamwidth of 105°, when the main beam is steered in broadside direction.

Detailed comparison of beam steering and beamwidth RA designs is presented in Table 2.4. It can be concluded that,

- There are very few RA designs that achieve beam steering and beamwidth tuning in a single antenna structure.
- The RA design presented in [25] is capable of achieving complete 360° coverage in the azimuth plane and beamwidth variability. However, the main beam and 3-dB beamwidth of the antenna are discretely switched.

Table 2.4. Performance comparison of the RA designs achieving beam steering and beamwidth variability in a single antenna structure.

Ref.	Antenna type	Operating frequency (GHz)	Size (mm^3)	Substrate	-10 dB bandwidth (%)	360° azimuth coverage	Beam steering (degree)	3-dB beamwidth (degree)	Peak gain (dBi)	Switches (number)	Pattern purity (Cross-polar.)
[100]	PRS	2	n/a	n/a	3	no	± 10 (H-plane)	18.7 to 22.4 (H-plane)	14.7	varactor (100)	< -12
[101]	Metamaterial	3.33	383.4×30.2×n/a	n/a	n/a	no	-49 to 50 (E-plane)	48, 37 (E-plane)	18	varactor (90)	n/a
[102]	Antenna with metal walls	3.7	43×43×19.075	n/a	10.8	no	-51, 54 (E-plane) -20, 20 (H-plane)	narrow wide	6	PIN (2)	n/a
[103]	Tunable parasitic	1.4	320×100×n/a	FR4	6.40	no	± 20 (H-plane)	60 to 130 (H-plane)	8.8	varactor (2)	< -15
[104]	Parasitic	3.5	100×100×6.8	Rogers	5.56	no	-17, 14	49, 105	7	PIN (8)	< -15
[25]	Parasitic pixel	5	60×60×10.813	Rogers	4	yes	± 40	40 (E-plane), 100 (H-plane) 100 (D-plane)	8	PIN (6)	< -20

It is observed that most of the PRA designs reported in the literature are linearly polarized. Pattern reconfiguration with CP is a difficult task to accomplish and is found to be very limited in the literature. Wireless communication applications need RA capable of radiating waves in more than one steering angle with polarization agility. Techniques used to realize CP beam switching, as shown in Figure 2.3 are based on spiral [105], waveguide [106], metasurface [107], parasitic [44], LWA [108], dipole [109], RFN [110], SIW [111], transmitarray [112], reflectarray [113] and DRA [114]. However, in these reported antenna designs, polarization reconfiguration is not achieved, and the main beam is steered with either LHCP or RHCP.

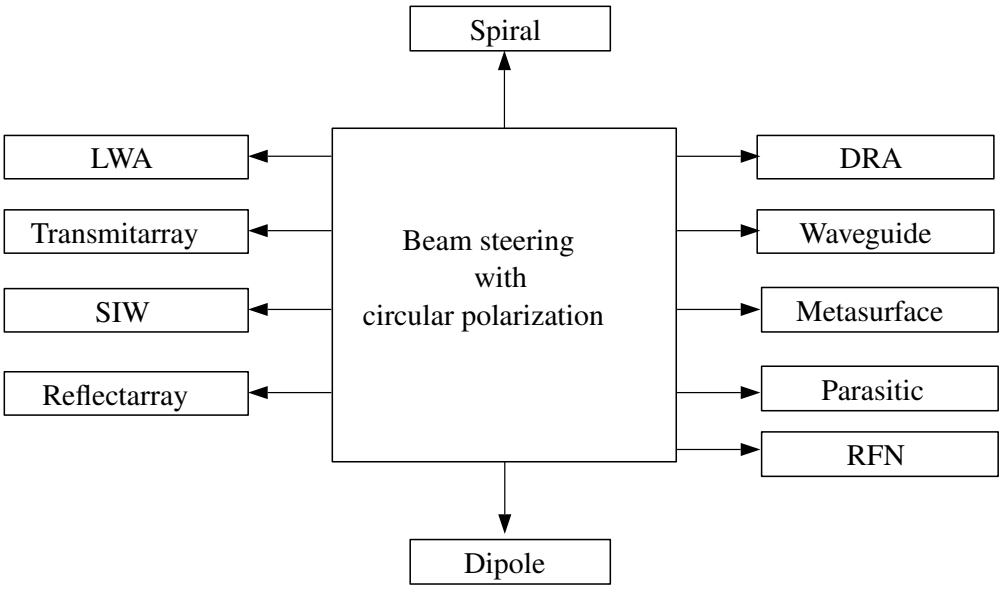

Figure 2.3. Techniques used to achieve beam steering with CP.

2.2.5 Circularly Polarized Beam Steering Antenna based on Parasitic Technique

The tunable parasitic patch size method is used in this thesis, and thus some of the designs [44, 115–119] that use this technique to perform CP beam steering are described briefly. A dual-feed parasitic antenna structure is proposed in [44] to achieve continuous beam scanning from -36° to 32° with RHCP characteristics. Tunable parasitic DRAs terminated with varactor diodes are used in [115] to realize RHCP beam scanning from -22° to 22°. An ESPAR antenna presented in [116] provides an RHCP beam steering over a complete azimuth plane. In [117], a shorting pin is connected between the parasitic elements and the ground plane to obtain LHCP discrete beam switching. In [118], parasitic elements are placed along the diagonal plane of the driven element to cover the complete azimuth plane. In [119], circular patch and several parasitic elements are used to attain beam steering with RHCP.

Detailed results of the CP beam steering antennas based on parasitic technique are summarized in Table 2.5. It should be noted that,

- In the above mentioned reported designs, polarization reconfiguration is not achieved. Main beam is steered with either RHCP [44, 115, 116, 119] or LHCP [117, 118].

2.2.6 Variation in Direction and Shape of the Radiation Pattern with Polarization Reconfiguration

In this section, the RA designs radiating in forward or backward direction and producing different radiation patterns along with the polarization reconfiguration are discussed. The antenna designs achieves broadside/conical pattern in [14, 120–122], omnidirectional pattern in [123–128] and broadside/backfire radiation pattern in [16, 129–131].

A square-ring radiating patch and four shorting walls are used in [14] to produce two complementary radiation patterns with dual orthogonal polarization. This antenna operates in two modes normal patch and monopolar patch. The antenna radiates in broadside direction with LVP and LHP polarization. The conical radiation pattern is obtained with LPθ polarization. This antenna achieves -10 dB impedance bandwidth of 7.2%, 6.4%, and 9.4% in the LVP, LHP, and LPθ polarization respectively. Peak gain of the antenna in broadside and conical direction is 5.5 dBi and 3 dBi, respectively.

A reconfigurable metamaterial antenna proposed in [120] achieves LP conical pattern and CP broadside pattern by controlling switching conditions on the feed network. This antenna attains -10 dB impedance bandwidth of 2.1% and 41% in the LP and CP mode respectively. The 3-dB AR bandwidth achieved in the CP mode is 14%. Peak gain of the antenna in LP and CP mode is 2.1 dBi and 7.9 dBi respectively.

A microstrip antenna with polarization diversity and pattern selectivity is proposed in [132]. This antenna overcomes the limitations of the antenna design presented in [120]. It is operated with a single feed and works in two modes normal patch and monopolar patch. The antenna produces RHCP with broadside radiation patterns and LP with a conical radiation pattern.

In [121], a circular patch with shorted conductive via is used to produce multiple LP for broadside pattern and single polarization for conical pattern. This antenna operates at 2.45 GHz with a peak gain of 6.05 dBi and 4.39 dBi for the broadside and conical radiation pattern, respectively.

Table 2.5. Performance comparison of the parasitic antennas designs realizing CP beam steering.

Ref.	Operating frequency (GHz)	360° azimuth coverage	Main beam elevation plane (degree)	Polarization	−10 dB bandwidth (%)	3-dB AR bandwidth (%)	Peak gain (dBic)	Substrate	Size (mm^3)	Switches (number)	Steering type
[44]	2.45	no	−36 to 32	RHCP	2.04	2.04	8.1	Rogers	150×100×3.175	varactor (4)	continuous
[115]	10.5	no	−22 to 22	RHCP	14.17	3.97	6.6	Rogers	45×45×0.508	varactor (4)	continuous
[116]	2.45	yes	omni & 45	RHCP	2	n/a	3	Rogers	25.37 (diameter) 0.81 (thickness)	PIN (16)	discrete
[117]	30	no	15, −15, 0, −20	LHCP	13.2	13.2	10.5	Rogers	15×15×0.941	PIN (4)	discrete
[118]	2.66	yes	25	LHCP	n/a	n/a	7	ϵ_r = 2.6	160×160×2.4	Single Pole Three Throw (SP3T)	discrete

A 2×2 stacked annular ring pattern and polarization RA array is proposed in [122]. The antenna produces broadside radiation with ±45° and ±135° polarization. It also generates a conical radiation pattern with LVP and LHP. This antenna achieves an overall impedance bandwidth of 13.66%. Peak gain of the antenna in broadside and conical direction is 12.5 dBi and 6.8 dBi, respectively.

A reconfigurable stacked square microstrip antenna proposed in [123] achieves pattern and polarization diversity at two different operating frequencies. The antenna produces a high gain directional pattern with RHCP at a higher frequency and low gain omnidirectional pattern with LP at lower operating frequency. However, this antenna has a large profile due to stacked design and complex structure due to dual ports.

In [124], center-shorted microstrip patch is used to realize pattern and polarization reconfiguration. The antenna radiates in broadside direction with two orthogonal LP and produces omnidirectional radiation with LVP. The overall impedance bandwidth of the antenna is 1.5%. This antenna has a peak gain of 6.2 dBi and 3.7 dBi for the broadside and omnidirectional radiation pattern, respectively.

A microstrip-fed truncated monopole antenna is proposed in [125] to attain pattern and polarization reconfigurability. This antenna produces omnidirectional patterns in different planes with dual orthogonal LP.

A compact CPW-fed RA composed of four radiating patches is proposed in [126], which achieves frequency, polarization, and pattern diversity. As the antenna polarization changes from RHCP to LHCP, the radiation pattern rotates from 0° to 180°.

A PIFA proposed in [127] produces an omnidirectional pattern in orthogonal planes with LHP and LVP. Peak gain of the antenna in LHP and LVP is 1.2 dBi and 4.2 dBi, respectively.

Back-to-back coupled patches fed by rat-race coupler are used in [128] to achieve pattern and polarization reconfiguration. The antenna radiates with two orthogonal linear ±45° slanted polarization, each with two dipole-like patterns, one covering 360° in the horizontal plane and the other in elevation. However, this antenna needs an external steering network to switch the antenna configuration. Gain of the antenna for configurations A, B, C, and D varies from −0.7 to 2.7 dBi, −5.7 to 3.2 dBi, −2.4 to 2.1 dBi, and −4 to 3.4 dBi respectively.

A sandwich-like RA structure with two crossed slots in the ground plane has been proposed in [129] to radiate the main beam of the antenna in forward and backward direction with +45° and −45° slanted polarization. However, this work leads to low reconfigurability and provide less number of operating modes with comparatively similar characteristics.

A cavity-backed slot antenna is proposed in [16] to achieve compound reconfiguration with frequency, pattern, and polarization agility. Two crossed slots loaded with switches on the surface of the SIW cavity are used to realize compound reconfiguration. The radiation pattern of the antenna can be reconfigured between forward and backward direction with LVP, LHP, LHCP, and RHCP polarization. For the LP state, frequency of the antenna can be tuned between three states, whereas for CP mode frequency is tuned between two bands. The proposed antenna has the advantage of achieving compound reconfiguration with a comparatively smaller size.

A cuboid quadrifilar helical antenna operating at 0.9 GHz is presented in [130] to achieve pattern and polarization reconfiguration. The PIN diodes on the radiator and feeding network are controlled to achieve orthogonal CP with radiation pattern switched between broadside and backfire. This antenna has the advantage of achieving 36.2% impedance bandwidth and 22% 3-dB AR bandwidth. Peak gain of the antenna in broadside and backfire direction is 3.8 dBic and 4.7 dBic, respectively.

In [131], 2×2 SIW ring slot antenna array is proposed to achieve pattern and polarization reconfiguration. The antenna radiates beam in four different directions with two orthogonal LP.

Table 2.6 summarizes detailed results for pattern and polarization RA designs radiating in different directions and producing different beam shapes. It can be observed that,

- The antenna designs presented in [14, 120–129] has a limitation that the pattern and polarization cannot be independently reconfigured, which significantly limits diversity provided by the compound RA.
- Reported designs in [16, 130, 131] have the advantage of achieving independent pattern and polarization reconfiguration. However, in [16], the overall impedance and AR bandwidth for each state is less than $< 4\%$. Also, this antenna needs 48 PIN diodes, which increases power consumption, loss, and complicates the DC biasing network.
- Limitation of a certain pattern and polarization RA in which the radiation beam is scanned within a limited range is overcome in [130] by radiating the main beam in broadside and backfire direction. However, this antenna has a high profile and non-planar design.

Table 2.6. Performance comparison of the pattern and polarization RA designs based on direction and shape of the radiated beam.

Ref.	Antenna type	Operating frequency (GHz)	Radiation pattern	Polarization	−10 dB bandwidth (%)	3-dB AR bandwidth (%)	Peak gain	Size (mm^3)	Switches (number)
[14]	Square-ring patch	2.44	broadside conical	LVP, LHP LPθ	7.2, 6.4 9.4	-	5.5 3	100×100×0.6	PIN (4)
[120]	Metamaterial	2	conical broadside	LP CP	2.1 41	- 14	2.1 7.9	100×100×5	copper strips (12)
[121]	Circular patch with vias	2.45	broadside conical	multiple LP 1 polarization	2.5	-	6.05 4.39	80 (diameter) 1.52 (thickness)	PIN (16)
[122]	2×2 stacked annular ring array	2.4	broadside conical	±45, ±135 HP, VP	13.66	-	12.5 6.8	200×200×7	PIN (16)
[123]	Stacked square antenna	0.67 1.75	omnidirectional broadside	LP RHCP	7.3 15.8	- 10	3.9 7.5	130×130×10	PIN (3)
[124]	Center shorted microstrip patch	3.67	broadside omnidirectional	LP (ϕ = 0 & 90) VP	1.5	-	6.2 3.7	n/a	PIN (12)
[125]	Microstrip truncated monopole	2.4	omnidirectional in different planes	LVP LHP	4.1	- -	−1.1	19×19×1.6	copper strips (2)

Continued on next page

Table 2.6 – *Continued from previous page*

Ref.	Antenna type	Operating frequency (GHz)	Radiation pattern	Polarization	−10 dB bandwidth (%)	3-dB AR bandwidth (%)	Peak gain	Size (mm^3)	Switches (number)
[126]	CPW-fed monopole	5.81 5.07 5.09 5.11	omnidirectional in different planes	LP LP LHCP RHCP	22.54 23.66 44.01 33.85	- - 38.8 33.66	2.9 3.4 3.7 3.5	16×16×2.1	copper strips (3)
[127]	PIFA monopole	2.4	omnidirectional in different planes	HP VP	8.4	-	1.2 4.2	50×50×1.52	PIN (1)
[128]	coupled patches fed by coupler	2.56	omnidirectional in different planes	±45	n/a	-	3.4	n/a	-
[129]	Sandwich-like structure with two crossed	2.5	broadside backfire	+45 −45	n/a	-	n/a	50×50×4	PIN (8)
[16]	Cavity-backed antenna	2.29 2.31	forward, backward	LVP, LHP LHCP, RHCP	≈2 ≈3.5	- ≈2.35	4.7	135×122×1.575	PIN (48)
[130]	Cuboid quadrifilar helical antenna	0.9	broadside, backfire	LHCP, RHCP	36.2	22	3.8, 4.7	87×87×83	PIN (32)
[131]	SIW ring-slot 2×2 array	5.8	beams in four directions	2 orthogonal LP	2.59	-	11.6	131.6×65.8×4.9	PIN (2)

2.2.7 Beam Steering with Linear Polarization Reconfiguration

This section presents the performance comparison of the RA designs capable of achieving beam steering with multiple LP operating states.

In [133], a cavity-backed proximity-coupled feed network and reconfigurable parasitic elements are used to realize beam steering with LP. This antenna achieves three different LPs in $\phi = 0°$, $45°$ and $90°$ planes. Main beam of the antenna is discretely switched to $20°$, $0°$, and $-20°$ in H-plane for each polarization state.

A cross patch antenna with one driven and four parasitic elements is presented in [134]. A Shorting switch connected between the patch and ground plane is used to switch the main beam direction. This antenna radiates in six different directions in the azimuth and elevation plane with LHP or LVP. The polarization reconfiguration is achieved by feeding the driven element with two feed probes. This antenna works according to the microstrip Yagi principle with parasitic elements that can be used as director or reflector.

A pattern and polarization RA presented in [135] generates two different LP and one diagonal polarization. By changing the bias voltage of PIN diodes on the parasitic elements, five different beams are produced in each polarization state.

An electrically actuated liquid-metal pattern and polarization reconfigurable dipole antenna is presented in [136]. It provides null steering with five discrete LP $0°$, $\pm 45°$, and $\pm 90°$ at an operating frequency of 1.579 GHz.

A Fabry-Perot cavity antenna with a reconfigurable PRS is proposed in [137] to achieve a 2-D beam steering with LP. The LVP and LHP are produced by aperture coupled patch antenna, and the beam steering is realized by controlling the reflection phase distribution of PRS by using PIN diodes.

Detailed results of the antenna designs achieving pattern and polarization reconfiguration with LP are summarized in Table 2.7. It can be observed that,

- The RA designs presented in [133–137] achieve discrete beam switching.
- In [133], the radiated beam is switched only in H-plane with limited steering capability from $-20°$ to $20°$.
- In [134], three different prototypes corresponding to mode 1, 2, and 3 are fabricated using copper as a shorting switch.
- The antenna design presented in [135] suffers from drawbacks such as the structure is non-planar, since the parasitic element is placed in the vertical plane and radiating patch in the

horizontal plane. Also, the radiated beam of this antenna cannot be steered towards broadside direction, and it has a very narrow impedance bandwidth.

- The RA design proposed in [137] needs 144 PIN diodes, which complicates the DC biasing network.

2.2.8 Beam Steering with Circular Polarization Reconfiguration

A pattern and polarization RA proposed in [138] consists of a metasurface and a slot antenna. This antenna achieves a discrete beam switching from -20° to 20° with LHCP and RHCP, at an operating frequency of 5 GHz. Overall impedance bandwidth of the antenna is 2%, and peak gain is 8 dBi. In [139], 2×2 patch antenna array is used to achieve independent polarization reconfiguration and beam switching. Radiated beam of the antenna covers the complete azimuth plane with LHCP and RHCP. Main beam of the antenna is switched to $\theta = \pm 16^\circ$, $\pm 16^\circ$, $\pm 28^\circ$, and $\pm 28^\circ$ for $\phi = 0^\circ$, 90°, 45°, and 135° respectively. This antenna uses a spatial phase technique to enhance AR bandwidth. The antenna achieves a peak gain of 10.5 dBi at an operating frequency of 4.8 GHz. Overall impedance and AR bandwidth of the antenna is 9.07%. Detailed results of the antenna designs [138, 139] are summarized in Table 2.8.

2.2.9 Beam Steering with Linear and Circular Polarization Reconfiguration

The pattern and polarization RA designs described in Section 2.2.7 and Section 2.2.8 provide beam steering with LP and CP, respectively. In this section, RA designs realizing beam steering with LP as well as CP are discussed in detail.

In [140], mutual coupling between the driven and four circular parasitic elements is used to realize pattern and polarization reconfiguration. For LP mode, the main beam is directed to broadside, 4°, and $\pm 19^\circ$, whereas with LHCP, the main beam is switched to $\pm 10^\circ$.

The RA with a parasitic patch layer is presented in [141], to realize discrete beam switching with LP and CP. The beam switching is obtained by utilizing mutual coupling between the driven and parasitic elements. The CP is obtained by making rectangular slits on the parasitic elements. Main beam of the antenna is discretely switched to -30°, 0°, and 30° with LP and CP.

A reconfigurable loop antenna consisting of four switched parasitic elements is reported in [142] to produce beam switching in LP, LHCP and RHCP states. In LP operating mode main beam of

Table 2.7. Performance comparison of the pattern and polarization RA designs achieving beam steering with multiple LP.

Ref	Antenna type	Operating frequency (GHz)	360° azimuth coverage	Main beam elevation plane (degree)	Polarization	−10 dB bandwidth (%)	Peak gain (dBi)	Size (mm^3)	Switches (number)	Steering type
[133]	Cavity-backed proximity coupling	11	no	−20, 0, 20	LP 0°, 45°, 90°	n/a	8.12	32×32×10.016	PIN (10)	discrete
[134]	Parasitic antenna	10	no	3 beam patterns	HP, VP	n/a	6.7	22×22×0.787	copper strips (4)	discrete
[135]	Parasitic antenna	2.4	yes	45	LVP, LHP, diagonal LP	≈0.8	3.5	150×150×29	PIN (8)	discrete
[136]	liquid-metal dipole antenna	1.579	no	null steering	five discrete LP 0°, ±45°, ±90°	n/a	2.08	n/a	liquid-metal	discrete
[137]	Fabry-Perot with PRS	5.5	yes	0, 10, −10	LVP, LHP	≈3.6	9.7	100×100×28	PIN (144)	discrete

Table 2.8. Performance comparison of the pattern and polarization RA designs achieving beam steering with CP.

Ref	Antenna type	Operating frequency (GHz)	360° azimuth coverage	Main beam elevation plane (degree)	Polarization	−10 dB BW (%)	3-dB AR BW (%)	Peak gain	Size (mm^3)	Switches (number)	Steering type
[138]	Metasurface	5	no	−20, 0, 20	LHCP, RHCP	2	2	8	78×78×2.388	PIN (32)	discrete
[139]	Truncated patch with sequential feeding	4.8	yes	broadside, ±16, ±28	LHCP, RHCP	9.07	4.16	10.5	100×100×4.624	PIN (12)	discrete

the antenna can be switched to $\pm 15^{\circ}$ and $\pm 25^{\circ}$. Whereas in LHCP and RHCP operating mode main beam is directed to $+30^{\circ}$ and -30°, respectively.

A rhombus-shaped compound RA is proposed in [143]. The antenna offers two operating frequencies of 5.2 and 5.8 GHz. Polarization can be switched between LP, circular, and $\pm 45^{\circ}$. However, all the mentioned polarizations are not obtained at both the operating frequencies i.e., at 5.2 GHz, $\pm 45^{\circ}$ slant polarization is achieved, and at 5.8 GHz, LP, LHCP, and RHCP are obtained.

Antenna design proposed in [144] uses truncated circular radiator, C-shaped parasitic elements, and perturbed rhombic slot to realize compound reconfiguration. This antenna achieves LP at both the operating frequencies, whereas LHCP and RHCP are obtained at 3.6 GHz and 5.8 GHz, respectively. The radiation pattern of this antenna can be switched to broadside, omnidirectional, and $\pm 30^{\circ}$ with LP. However, with LHCP and RHCP radiation main beam of the antenna is always directed in broadside.

A crossed Yagi patch antenna is proposed in [145] to achieve pattern diversity and polarization selectivity. The two identical reconfigurable linear Yagi-Uda patch arrays are placed orthogonal to each other around a single driven element. Main beam of the antenna is tilted in the elevation plane by approximately 35° for LP and CP configuration.

A parasitic layer of 6×6 metallic pixels is placed above the driven element in [15] to realize compound reconfiguration in terms of frequency, pattern and polarization. The antenna achieves LVP, LHP, LHCP and RHCP polarization. Main beam of the antenna is discretely switched to $\pm 30^{\circ}$ in both E-plane and H-plane. Frequency tuning of 12% to 25% is realized by changing the distance between the driven and parasitic elements.

A 1×4 phased array consisting of a circular patch with an annular microstrip ring is presented in [146]. Four varactor diodes are loaded on the ring to achieve frequency tuning from 1.5 to 2.4 GHz. RFN is used to obtain two orthogonal LP and CP. The antenna achieves beam steering of $\pm 28^{\circ}$ at 2.4 GHz and $\pm 52^{\circ}$ at 1.5 GHz.

In [147], a multi-directional beam and multi-polarization antenna is proposed. The antenna is operated in eight operating modes of LP pattern with narrow and wide beamwidths, LP with $\pm 20^{\circ}$ beam switching in E-plane and H-plane, LHCP and RHCP with wide 3-dB beamwidth and 3-dB AR beamwidth. This antenna has the advantage of achieving wide 3-dB AR beamwidth for LHCP and RHCP configuration.

Table 2.9 summarizes the results of antenna designs that attain pattern reconfiguration with LP and CP operating states. It is observed that,

- The antenna design presented in [141] achieves a narrow impedance bandwidth of $\sim$1%. Three prototypes corresponding to LP configuration are fabricated. Also, this antenna needs a large number of switches, which complicates the DC biasing network.
- In [143, 144] pattern and polarization of the antenna cannot be independently reconfigured. Also, in [143], broadside radiation is not obtained.
- In [145], two specific prototypes corresponding to LP and CP configuration are fabricated. Metal pads are used in fabricated prototype for the switched on and off condition.
- The antenna design reported in [15] has a large size, and 60 PIN diodes are needed, which complicates the DC biasing network. This antenna only realizes discrete beam switching, also complete 360° azimuth coverage is not obtained.
- The phased array developed in [146] is associated with a complicated feeding network, and beam steering is achieved only in the H-plane.
- RA design presented in [147] has certain limitations such as discrete beam switching, limited beam switching of $\pm$20°, complete 360° azimuth coverage is not realized and beam switching is not obtained with CP.

Table 2.9. Performance comparison of the pattern and polarization RA designs achieving beam steering with LP and CP.

Ref	Antenna type	Operating frequency (GHz)	360° azimuth coverage	Main beam elevation plane (degree)	Polarization	−10 dB BW (%)	3-dB AR BW (%)	Peak gain	Size (mm^3)	Switches (number)	Steering type
[140]	Tunable parasitic	10.3	no	broadside, 4, ±19, ±10	LP LHCP	6.3	- 2.57	n/a	n/a	copper strips (8)	discrete
[141]	Parasitic pixel layer	5.25	no	−30, 0, 30	LP, CP	≈1	n/a	8	60×60×2.05	copper strips (40)	discrete
[142]	Planar monopole-fed loop antenna	1.57	no	±15 ±25 L 30, R −30	LP LP LHCP, RHCP	4.4 1.9 3.5	- - 3.32	4.2	33×30×1.6	PIN (4)	discrete
[143]	Rhombic-shaped patch	5.2 5.8	no	±30	±45 LP, LHCP, RHCP	3.59 3.5	- 3.5	3	60×150×1.6	PIN (6)	discrete
[144]	Patch-slot antenna array	3.6 5.8	no	omni broadside broadside, ±30 broadside	Linear LHCP Linear RHCP	6.4 5.2	13.13 3.1	8.9	160×160×1.6	PIN (10)	discrete
[145]	Crossed-Yagi	4.02	yes	≈35	LVP, LHP LHCP, RHCP	5.96 5.91	- n/a	8.68	140×140×1.5	copper strips (12)	discrete
[15]	Parasitic pixel layer	2.7	no	±30	LVP, LHP LHCP, RHCP	2.8	n/a	4 dB (avg.)	240×120×7.5	PIN (60)	discrete
[147]	Planar patch with metal wall	3.3	no	±20 broadside	LP LHCP, RHCP	10.7	9.3	n/a	43×43×13.79	PIN (12)	discrete

2.3 Summary

In this chapter, various methods to achieve pattern reconfiguration with LP and CP are reviewed in detail. Advantages and limitations of the existing 1-D PRAs, 2-D PRAs, and beamwidth RAs are also discussed. The key points from the literature survey can be summarized as follows:

- The PRAs, based on the parasitic technique, achieves discrete beam switching with limited beam steering.
- The PRAs working according to the microstrip Yagi principle, have often used H-plane coupling to achieve beam steering. It is necessary to place parasitic elements along the E-plane and H-plane of the driven element to achieve 360° azimuth coverage.
- Most of the beamwidth RAs attain discrete beamwidth tuning either in E-plane or H-plane.
- From the literature survey, it is strongly felt that to achieve multiple functionalities in a single antenna structure is a difficult task. The challenge is also to design RA with a low profile, low complexity, low cost, and easy integration with the feed networks.
- There are very few antenna designs reported, which achieves continuous beam scanning and tunable beamwidth in a single antenna structure.
- The compound RAs capable of providing space and polarization diversity has a strong potential to improve the performance of wireless communication systems. It is observed that very few antenna designs address the challenge of realizing independent pattern and polarization reconfiguration.